2017-05-08

Proteomics of FACS-sorted heterogeneous Corynebacterium glutamicum populations

Harst, A

10.1016/j.jprot.2017.03.010
Journal of Proteomics

This is an accepted manuscript of an article published by Elsevier in Journal of Proteomics

(accepted March 13 2017) available at:

https://doi.org/10.1016/j.jprot.2017.03.010

==========

Proteomics of FACS-sorted heterogeneous *Corynebacterium glutamicum* populations

Andreas Harst1, Stefan P. Albaum2, Tanja Bojarzyn1, Christian Trötschel1, Ansgar Poetsch1,3

[1]Department of Plant Biochemistry, Ruhr-University Bochum, 44801 Bochum, Germany

[2]Bioinformatics Resource Facility, Center for Biotechnology (CeBiTec), Bielefeld University, Universitätsstraße 27, 33615 Bielefeld,

[3] School of Biomedical and Healthcare Sciences, Plymouth University, Plymouth PL4 8AA

Correspondence:

Dr. Christian Trötschel / Dr. Ansgar Poetsch

Ruhr-University Bochum

Universitätsstr. 150

D-44801 Bochum, Germany

E-mail: christian.troetschel@rub.de

ansgar.poetsch@rub.de

Fax: +49 (0) 234 32 14322

Keywords: *Corynebacterium glutamicum*, BCAA producer, cellular heterogeneity, FACS, proteome analysis, label-free quantification

ABSTRACT

The metabolic status of individual cells in microbial cultures can differ, being relevant for biotechnology, environmental and medical microbiology. However, it is hardly understood in molecular detail due to limitations of current analytical tools. Here, we demonstrate that FACS in combination with proteomics can be used to sort and analyze cell populations based on their metabolic state. A previously established GFP reporter system was used to detect and sort single *Corynebacterium glutamicum* cells based on the concentration of branched chain amino acids (BCAA) using FACS. A proteomics workflow optimized for small cell numbers was used to quantitatively compare proteomes of a *ΔaceE* mutant, lacking functional pyruvate dehydrogenase (PD), and the wild type. About 800 proteins could be quantified from 1,000,000 cells. In the *ΔaceE* mutant BCAA production was coordinated with upregulation of the glyoxylate cycle and TCA cycle to counter the lack of acetyl CoA resulting from the deletion of *aceE*.

ABBREVIATIONS

Branched chain amino acids (BCAA)
Peptide spectra matches (PSM)
Top 3 protein quantification (T3PQ)
Leucine responsive protein (LRP)
Fluorescence activated cell sorting (FACS)
Tricarboxylic acid cycle (TCA)
Pentose Phosphate pathway (PPP)

INTRODUCTION

The metabolic status of individual cells in microbial cultures can differ, and of particular interest for biotechnology are screening methods for phenotypes where productivity increases or inadvertently decreases. Cell-sorting methods in combination with proteomics could then be used to analyze the molecular background of this phenomenon. A requirement is a method to determine the concentration of a metabolite on the single cell level, for instance by fluorophore-staining [1] or GFP-reporter systems [2]. To pursue single cell analysis several techniques, such as flow cytometry, microfluidic chips and single cell genomics, were developed [3]. Most prominent is flow cytometry, where a directed laminar flow contains cells in small droplets which are aligned in a pearl chain-like manner. The liquid droplets pass through detectors which record the characteristics of each single cell. Cytomics is defined as multimolecular cytometric analysis combined with exhaustive information extraction from all measured cells [4]. Proteomic analysis of cell samples sorted by flow cytometry can thus be seen as a domain of cytomics. Proteomics provides an accurate and sensitive approach for comprehensive protein identification and monitoring of the physiological state of sorted cells. A first study combining flow cytometry and proteomics analyzed sorted subpopulations of *C. necator*, formed due to exposure to phenol, with 2D gels [5]. Furthermore, flow cytometry and MS were combined by using a filter based sample preparation method; here loss of cells was minimized by using the same filter membrane for storage and digestion. As proof of principle *P. putida* and *E. coli K12* cells were mixed and then sorted using flow cytometry and proteins sequentially identified by MS [6]. For satisfactory proteome coverage about $5x10^6$ bacteria were required.

The bacterium *Corynebacterium glutamicum* is a member of the family of actinomycetales and dominates industrial scale production of amino acids [7]. The production volumes range from 2.5 million tons of L-glutamate to 1.5 million tons of L-lysine per year. Also large amounts of the amino acid L-threonine and of the branched chain amino acids (BCAA) L-leucine and L-valine are produced [8]. For BCAA production a reporter system was constructed by combining *eyfp* with a *brnF* promotor, which allows to detect BCAA concentration on the single cell level: The BrnFE permease exports BCAA and is transcriptionally controlled by the Lrp protein which

is activated by binding of BCAA [9]. Increased levels of BCAA lead to expression of eYFP allowing effective sorting of cells with high BCAA concentrations [2].

Engineering efforts leading to increased L-valine production in *C. glutamicum* were centered on the deletion of the pyruvate dehydrogenase complex (PDHC) [10]**.** BCAA- producing strains are based on deletion of the *ΔaceE* gene coding for the PDHC subunit E1p leading to an increased accumulation of pyruvate [11]. Flux analysis of the *ΔaceE* strain already partially elucidated the carbon flows leading to an increased BCAA production [12], still the protein networks enabling increased BCAA production must be uncovered.

In this study, a method was developed to separate cells based on their content of a desired metabolite and to disclose differences in their metabolic networks by proteomics. The method was evaluated by characterizing differential abundance of proteins from a mixture of a BCAA-producing strain and a nonproducing wildtype of *C. glutamicum* cells. Comparison of proteomes allowed uncovering mechanisms that explain the differences in metabolite content and enable increased BCAA production.

MATERIALS and METHODS

C. glutamicum strains, media and culture conditions

C. glutamicum ATCC 13032 was used as a wild type strain [13], the *ΔaceE* mutant ([14];[10]) was used as BCAA production strain. A first pre-culture of *C. glutamicum* was inoculated with colonies from a fresh BHI agar plate (brain heart infusion, Difco™ BHI, BD, Heidelberg, Germany) and grown in 5 ml BHI liquid medium supplemented with 0.5% potassium acetate for 8 hours at a temperature of 30 °C and a shaking rate of 170 rpm. Afterwards, cells were washed with 0.9 % (w/v) NaCl and were transferred to 50 ml CGXII minimal medium with 4 % (w/v) glucose and 1.5 % potassium acetate [15]. The culture for comparison of the *ΔaceE* sensor strain and the WT was inoculated to an OD_{600} of 1.0 in this medium and *C. glutamicum* was grown at 30 °C for 48 hours in 500 ml shaking flasks in 50 ml medium. Cells were cultured overnight at 30 °C with a shaking rate of 120 rpm.

Table of Bacterial strains used in this work

Strains	Characteristics	Reference
C. glutamicum ATCC13032	*C. glutamicum* wild type (ATCC13032) and with chromosomally integrated Lrp sensor (integrated between cg1121-cg1122).	[13]
C. glutamicum ATCC 13032 ΔaceE sensor strain	*C. glutamicum* wild type with deletion of the E1p gene *(aceE)* of the PDHC and with chromosomally integrated Lrp sensor (integrated between cg1121-cg1122).	[2]

Flow cytometry measurements

Flow cytometry measurements were performed using a FACS Aria II cell sorter (Becton-Dickinson, Heidelberg, Germany) using a blue solid state laser (Sapphire™ 488-20) with an excitation wavelength of 488 nm and a power of 13 mW. Cytometer setup and performance tracking was performed with Cytometer Setup & Tracking Beads (bright (3 µm), mid (3 µm), and dim (2 µm) beads) labeled with a mixture of fluorochromes (Becton Dickinson, Heidelberg, Germany). EYFP fluorescence was detected via a 502-nm long pass and a 530/30-nm band-pass filter set. Data were recorded with the FACS Diva software 6.0 and were analyzed with the FlowJo flow cytometry analysis software 7.6.5 (Tree Star, Ashland, USA).

Cell sorting procedure

Cell sorting was performed in the four-way purity precision mode with flow rates ≤3 using the FACSAria II cell sorter. Drop delay was set with FACS™ Accudrop Beads (Becton Dickinson, Heidelberg, Germany) containing a single population of 6-µm particles that consist of a fluorophore that is excited at 670 nm and emits at 750 nm. Cells were sorted and collected on a 96-well plate containing a hydrophilic polyvinylidene fluoride (PVDF) membrane at the bottom (Millipore, Schwalbach, Germany) to an amount between $1x10^4$ and $1x10^6$ cells per filter membrane. The multi-dish plate was connected to a vacuum pump so that the buffer could be directly removed and cells could be concentrated on the filter membranes. Thereby, three replicates for each sample were performed. Filter membranes could be stored at -20 °C until cell disruption.

Cell lysis and protein digestion

Filter membranes containing bacterial cells were divided into smaller pieces and were dissolved in 32 µl dissolution buffer (25 mM ammonium bicarbonate, pH 7.8 containing 2 µl acetonitrile). Subsequently, cells were proteolytically digested with 8 µl trypsin (Promega, Mannheim, Germany) resulting in a working concentration of 0.25 µg/µL at 37 °C with continuous shaking at 400 rpm for 2 hours. Afterwards, cell debris and filter membranes were removed by centrifugation at 13,000 g for 10 minutes at RT. Supernatants were collected in a new tube and were stored up to one week at -20 °C.

Protein identification via 1D-nLC-ESI/MS

The lyophilized tryptic digests were re-suspended in buffer A (0.1 % v/v formic acid in water) by ultrasonication and subjected to mass spectrometric analyses, which were performed using a nanoAcquity UltraPerformance LC System connected to an auto-sampler equipped with a HSS T3 analytical column (1.8 µm particle, 75 µm x 150 mm) kept at 45°C, and a Symmetry C18 trap column (5 µm particle, 180 µm x 20 mm) (all Waters, USA) as well as a PicoTip Emitter (SilicaTip, 10 µm) from New Objective (USA) as a nanospray source, coupled to an LTQ Orbitrap Elite mass spectrometer from Thermo Fisher Scientific Inc. (USA). The LTQ Orbitrap was operated by instrument method files of Xcalibur (Rev. 2.2 SP1). The linear ion trap and Orbitrap were operated in sequence, i.e. after a full MS scan on the Orbitrap in the range of 300-2000 m/z at a resolution of 60,000, the 10 most intense precursors were subjected to CID

fragmentation (ion target value of 10,000, activation time of 10 ms, 400ms maximal inject time, 35 % normalized collision energy) and fragments detected in the ion trap. The heated desolvation capillary was set to 275 °C. Dynamic exclusion was enabled with a repeat count of 1 and a 45 sec exclusion duration window. Singly charged ions and ions of unknown charge state were rejected from MS/MS. Flow rate was set to 400 nl/min and spray voltage was set to 1.5-1.8 kV. Peptides were eluted from Trap column onto a separation column using a multi-step gradient of buffer A to buffer B (0.1 % v/v formic acid in acetonitrile). A 180 min gradient was used: (0-5 min: 99 % buffer A and 1 % buffer B, 5-10 min 99 %-94 % A, 10-161 min: 94 %-60 % A, 161-161.5 min: 60 %-14 % A, 161.5-166.5 min: 14 %-4 % A, 166.5-167.1 min: 99 % A, 167.1 min-180 min: 99 % A).

Database searches

All database searches were performed using SEQUEST algorithm, embedded in Proteome Discoverer™ (Rev. 1.3, Thermo Electron © 1998-2007), with a *C. glutamicum* ATCC 13032 database containing 3058 sequences, which was provided by Jörn Kalinowski from Bielefeld University [13]. Only tryptic peptides with up to 2 missed cleavages were accepted. No fixed modifications were considered. Oxidation of methionine was permitted as variable modification. The mass tolerance for precursor ions was set to 10 ppm; the mass tolerance for fragment ions was set to 0.8 amu. For search result filtering, a peptide FDR threshold of 0.01 (q-value) according to Percolator was set in Proteome Discoverer, and at least two unique peptides with search result rank 1 were required.

Label-free quantification

For Top 3 Protein Quantification (T3PQ) ([17]; [18]), the average area of the three unique peptides of a protein with the largest peak area was calculated by Proteome Discoverer. This quantification method was used to obtain the area values for the data presented here. The mass spectrometry proteomics data have been deposited to the ProteomeXchange Consortium via the PRIDE [1] partner repository with the dataset identifier PXD005812 and 10.6019/PXD005812.

Bioinformatics

194 Samples were standardized based on a z-score normalization, i.e. for each sample and
195 replicate the respective mean value and standard deviation was calculated and used to
196 normalize each measurement. Afterwards an ANOVA was calculated comparing all replicate
197 measurements of sample P1 against sample P2. Aiming at an utmost comprehensive set of
198 potentially interesting candidate proteins, an adjustment of p-values to compensate for the
199 multiple testing situation has deliberately been omitted. Principal component analyses were
200 performed comparing P1 and P2. At this only proteins with complete series of measurements
201 were taken into consideration with replicate measurements being combined by calculating
202 their mean value. All analyses were carried out in the R environment for statistical computing
203 and graphics using standard packages (“stats”, “graphics”) [19].
204
205

RESULTS

Workflow for small cell number proteomics with FACS-sorted *C. glutamicum*

Protein Identification in small cell number samples

A robust, yet sensitive proteomics workflow is required for protein identification in small cell number samples or subpopulations acquired by cell sorting. The low protein content of single *C. glutamicum* cells in the range of 0.13 pg (own unpublished result) to 0.2 pg (calculated for *E. coli* from [20]) makes it obvious that a very sensitive proteomics method has to be used. The filter-based cell disruption approach minimizes loss of cells and allows for sequential sample preparation in the same environment and can be combined with different MS proteomics setups [6]. This method was used to establish the correlation of sorted cells to protein identifications by sorting 1,000,000, 100,000 and 10,000 *C. glutamicum* WT cells and subsequent preparation. From 1,000,000 cells (about 130 ng) 489 proteins were identified, 100,000 cells led to identification of 107 proteins and 10,000 cells led to identification of 61 proteins (Fig. 1). As the discrepancy between 1,000,000 cells and lower cell numbers was too large, optimization of MS methods was only performed for 1,000,000 cells, where identification was improved by increasing the filling time from 150 to 400 ms to better account for the low amount of sample loaded. This optimization led to protein identification rates on average close to 650 proteins.

Identified proteins were quantified using spectral counting and T3PQ. To assess correlation of quantification results between both methods principal component analysis was performed for a combined dataset from several experiments. Principal components were determined and used to represent the covariance in the z-standardized dataset. For PSM and T3PQ quantification similar variation between experiments was observed for the first and second principal components (data not shown). Based on these results we decided to preferably use T3PQ quantification for presenting our data in the following experiments.

Proteomic evaluation of FACS sorting based on the metabolic state of *C. glutamicum* cells. Cytometric analysis shows that cells of *C. glutamicum* WT strain and *ΔaceE* mutant exhibited

different levels of eYFP fluorescence. For the FACS sorting experiment cells were sampled after 12 hours when increased eYFP fluorescence generated by the Lrp sensor is detectable in L-valine producing *ΔaceE* strains. Active fluorescence caused by the Lrp sensor is required to distinguish BCAA-producing cells from cells not producing BCAA. To demonstrate that this workflow can successfully be applied to uncover proteome differences *ΔaceE* and WT strain cells were sorted from separate cultures first. For the eYFP fluorescence most cells from the *ΔaceE* strain show fluorescence intensity between 10^3 and 10^5, while most WT cells only exhibit fluorescence levels below 10^2 **(Fig. 2 b)**. Of note, the cells of the WT and *ΔaceE* strain do not show a distinction in cell size and cell morphology as the FSC-A readout between both populations demonstrates. Therefore, the main distinction between these cells is not a change in morphology but the physiological changes leading to increased BCAA production. The reliability of the *ΔaceE* cell sorting procedure applied here was established in a previous study by sorting *ΔaceE* single cells onto agar plates from a mixture with *C. glutamicum* WT only containing 1% *ΔaceE* strain cells. Strains were distinguished by the small colony phenotype of *ΔaceE* and subsequent colony PCR showing a 95% correct sorting efficiency for *ΔaceE* [2]. The sorted cells were subjected to the filter based sample preparation approach for proteome analysis.

Principal component analysis of quantitative proteome data was performed to assess, if the proteome of *ΔaceE* and WT cells sorted from mixed cells shows the same features as *ΔaceE* and WT proteomes extracted from separate cultures (Fig, 2c.) to validate FACS sorting. For the first **(Comp. 1)** and second principal component **(Comp 2)** the proteome of *ΔaceE* cells sorted from the mixed culture displayed an almost identical orientation of its dataset to the *ΔaceE* dataset from separate cultures. Additionally, ANOVA was done to find individual proteins that may differ in their concentration between samples from mixed and separate cultures of the respective strains (Supp. Table 1). Only 97 of 728 identified proteins showed a p-value below 0.05 and thus differed in amount between mixed and separated samples. Still these proteins did not change significantly according to the adjusted p-value. Based on PCA and ANOVA, it can be concluded that the proteome of the WT cells sorted from the mixed culture and the WT cells from the separate cultures behaved in the same fashion. Hence, FACS could successfully separate cells based on metabolite content and mixing of the two cultures

did not affect the proteome.**Characteristic differences between WT and *ΔaceE* strain proteomes**

It was our intention to demonstrate that the small cell numbers obtained by FACS separation allow for comprehensive proteome comparison of *C. glutamicum*. Here, this would allow characterizing physiological features of BCAA production in *C. glutamicum ΔaceE* in comparison to no production in *C. glutamicum* WT, both cultivated for 12 hours. After FACS, in total 960 proteins were identified and quantified across all replicates from separate samples. 701 of these proteins were identified in the *ΔaceE* strain as well as in the WT strain. Only 56 proteins were exclusive to the WT strain and 203 proteins to the *ΔaceE* strain. Label free quantification of the identified proteins enables interpretation of the changes in metabolic pathways given in detail below (Table 1).

In the mutant the glycolysis pathway is utilized as a main energy source, also providing precursors for the production of BCAA. Unsurprisingly, the largest decrease of an enzyme in the mutant was reported for the AceE subunit of the pyruvate dehydrogenase complex with a complete disappearance of the enzyme. Glycolytic enzymes as glyceraldehyde-3-phosphate dehydrogenase (GAP) and enolase showed decreased abundances in the *ΔaceE* mutant, reflected in a regulation factor of -0.15 and -0.33, respectively. To increase carbon supply for glycolysis the phosphoglycerate dehydrogenase, an enzyme directing carbon away from the glycolytic pathway, was downregulated in the *ΔaceE* mutant by -0.41.

Deletion of the pyruvate dehydrogenase is accompanied by upregulation of the TCA cycle and the glyoxylate cycle. Disappearance of the pyruvate dehydrogenase complex leads to a decline of acetyl-CoA levels in the *ΔaceE* mutant (Bartek et al. 2011). Enzymes of the TCA also being part of the glyoxylate cycle were upregulated in the *ΔaceE* strain (Fig. 3). Based on the regulation factors for citrate synthase (CS), aconitase (ACO), isocitrate dehydrogenase (IDH) and succinyl CoA synthetase (SUC) an increase in abundance in *ΔaceE* was found. The only enzymes with a decrease in the mutant were malate dehydrogenase (MDH) and fumarate hydratase (FUM) both having a regulation factor of -0.39, awhile the counterpart of MDH for this reaction malate quinone oxidase (MQO) was slightly upregulated (0.24). Glyoxylate cycle enzymes show strong overexpression in the *ΔaceE* mutant, especially isocitrate lyase (IL) with

301 a regulation factor of 1.13 strongly increased in the mutant. Malate synthase (MS) too was
302 upregulated as shown by the regulation factor of 0.53. Upregulation of these enzymes is
303 similar to that of the acetate fixation pathway where acetate kinase and phosphate
304 acetyltransferase as well as the succinyl acetate CoA transferase (SCOA) were upregulated.
305 Considerable upregulation occurred for the pyruvate carboxylase reaction, which replenishes
306 oxaloacetate from pyruvate while consuming one molecule of ATP, too. Apparently, in
307 response to absence of the pyruvate dehydrogenase complex reaction the TCA was provided
308 with carbon from replenishing pathways which consume energy and provide less NADH.
309
310

DISCUSSION

Workflow for small cell number proteomics with FACS-sorted *C. glutamicum*

A prerequisite for successfully performing proteomics with small cell numbers is a workflow that minimizes sample loss. The method of Jehmlich et al. [6] was chosen as it allows combining several sample processing steps, e.g. as lysis and digestion, to take place in one compartment. Aiming to further optimize the procedure for our experiments, we found that the use of an increased filling time was the key for improved proteome coverage. The maximal number of protein identifications our small cell number proteomics method can attain was calculated as the mean of three 1,000,000 cells samples of the *C. glutamicum* WT proteome and could be calculated to be 863 proteins, this equals a 28.7% proportion of the total proteome. In a 2013 study for 5,000,000 *P. putida KT2440* cells a total of 743 unique proteins were identified in 4 replicates, equaling a proportion of 13.7% of the global proteome [21]. Combining the sample processing developed by Jehmlich et al. with our mass spectrometry setup and the improvements in the measurement methods enabled us to identify proteins in small subpopulations for the first time for the organism *C. glutamicum*. Small cell number proteomics methods developed for eukaryotes [21] were not tested for our experiments as the cell wall of prokaryotes shows much higher level of rigidity in comparison to eukaryotes, which requires a harsher lysis procedure.

Proteomic evaluation of FACS sorting based on the metabolic state of *C. glutamicum.* In this study we used an approach that relies on sorting of fluorescent cells containing the LRP sensor system reporting on BCAA concentrations to assess the changes in the proteome leading to BCAA production. Fluorescent cells are a prerequisite for FACS sorting, therefore in early studies DAPI staining of cellular DNA was used to separate *E. coli* and *P. putida* cells displaying by way of proteomics that this sorting process is very efficient [6]. Furthermore in a 2013 study *P. putida* cells producing a fluorescent eGFP protein fused to the *styA* gene were sorted based on eGFP fluorescence and forward scatter. Using the two parameters cells were sorted into a group showing no fluorescence due to high DNA synthesis, as well as into a group of sorted fluorescent cells with a high forward scatter exhibiting a high accumulation of the styA protein and decreased cell cycle activity [21]. In contrast to these previous approaches the novelty of

our approach lies in sorting and selecting cells based on their metabolic status, here production or no production of the small molecule BCAA. This enables proteomics for the direct interrogation of changes in the metabolic pathways and other cellular functions in producing and non-producing subpopulations.

Assessment of FACS sorting efficiency with proteomics. The LRP reporter sensor system is known to be very robust in reflecting different levels of BCAA production as well as its specific fluorescence 2 times stronger than unspecific background fluorescence, hence being a good marker for BCAA nonproduction using cytometric methods [2]. However, the efficiency of FACS sorting using such a metabolite concentration reporter system remained to be verified on the molecular level, as done here for the proteome. For this purpose, the small cell number proteomes of WT *C. glutamicum* cells and *ΔaceE* cells were analysed from pure cultures and FACS-separated mixed cells to corroborate differences in physiology indicated by fluorescence as well as by PCA and ANOVA analysis of the proteomes. The proteomes of BCAA nonproducing WT from the mixed culture as well as cells sorted from independent cultures are very similar, same is true for the BCAA producing *ΔaceE* cells. Overall, PCA and ANOVA validated that the differences in proteomes was larger between strains than between mixed samples and samples from pure cultures of the same strain. This fits well to the results of a previous study by [6] where it was shown that *E. coli K12* and *P. putida KT2440* cells can be sorted with high specificity. Thus, FACS can efficiently sort cells without the sorting process affecting strongly the proteome status. This has already been shown for prokaryotic proteomes by [6]. Whereas Jehmlich used fixation of the cells, we assumed that our short sorting time should hardly affect the proteome, hence fixation could be omitted for proteome studies. Moreover, the insignificant differences between the proteomes from sorted and pure cultures demonstrate that properly designed eYFP fluorescence reporter systems can faithfully discriminate the physiological state – at least on the proteome level - in cell mixtures. This also implies that in addition FACS sorted cells can be used to reliably assess regulation mechanisms between producing and nonproducing strains or subpopulations.

Characteristic differences between WT and *ΔaceE* strain proteomes

C3 and C4 stockpiles in the TCA are replenished using malate provided by the glyoxylate cycle. ANOVA analysis of the proteomes substantiated that the proteins involved in central carbon metabolism as well as in amino acid metabolism are significantly regulated towards the metabolisation of acetate. The enzymes adding most to the variation between *ΔaceE* strain proteome and WT strain proteome are isocitrate lyase (Cg2560), citrate synthase (Cg0949) and phosphate acetyltransferase (Cg3048). This is in line with previous research, which showed that in case of removal of precursors from the TCA cycle, this cycle is refilled by the glyoxylate cycle [22] as happens in the *ΔaceE* strain, thus the TCA and glyoxylate cycle in the *ΔaceE* strain are upregulated in comparison to the WT in contrast to *E. coli* where the glyoxylate cycle is repressed when glucose and acetate are both present. This enables parallel metabolization of acetate and glucose in *C. glutamicum* [22]. A previous study found that during growth on glucose+acetate the glyoxylate cycle is used to replenish the malate pool which is needed for the TCA [22]. Also induction of TCA cycle gene transcripts in WT *C. glutamicum* cells only grown on acetate was reported in 2002 [23]. Under these conditions acetyl-CoA is predominantly produced from acetate [22]. This is corroborated by metabolic flux data, as in PDHC deficient strains fed with labeled glucose and unlabeled acetate a large fraction of unlabeled TCA intermediates persists [12]. Upregulation of enzymes belonging to the glyoxylate cycle provide C3 and C4 molecules for anabolic reactions in the cells [24].

Upregulation by the RamB transcriptional regulator can be found for several pathways of acetyl-CoA synthesis bypassing the pyruvate dehydrogenase complex. A genetic mechanism for the upregulation of the IL and MS genes taking part in the glyoxylate cycle via repression by RamB has been established [25]. Also RamB binding motifs were computationally identified in front of the genes for pyruvate carboxylase and citrate synthase. Pyruvate carboxylase as well provides intermediates for the TCA cycle by synthesizing oxaloacetate from pyruvate. Our data corroborates concomitant possible induction of pyruvate carboxylase and citrate synthase by RamB as suggested by computational detection of binding motifs in the *C. glutamicum* WT genome [25]. Previous studies show these proteins are already upregulated in the WT due to the co-metabolization of acetate and glucose. Still we detect a higher abundance of these proteins in the *ΔaceE* evidencing an influence of the acetyl-CoA pool on the level of gene expression controlled by RamB. Another bypass using the up-regulated SCOA,

where regulation is unknown, can convert acetate to acetyl-CoA by transfer of the CoA group from succinyl-CoA [26].

The AHAS enzyme, a central step in BCAA synthesis, showed only low upregulation in *ΔaceE*. This low level upregulation is mirrored by flux data where a low level increase of carbon flux could be detected when comparing WT and *ΔaceE* [12]. In *ΔaceE* an increased pool of pyruvate is available [27]. This raised concentration is favourable for the acetohydroxyacid synthase (AHAS) enzyme which has a high K_m for pyruvate at 8.3 mM [28]. The synthesis pathways of leucine, isoleucine and valine are regulated at the AHAS reaction step by feedback inhibition with BCAA [28].

Regulation of enzymes utilizing pentose phosphate pathway and glycolysis for increased BCAA synthesis. The proteome data for the carbon metabolism points to differential regulation between *ΔaceE* and the WT strain. A decreased glucose consumption has been documented for the *ΔaceE* strain [12], also we found a slight downregulation of GAPDH and a stronger decrease of the glycolytic enzyme enolase. Still for the enolase reaction a strong increase in flux for the *ΔaceE* strain has been measured [12], suggesting allosteric regulation and/or PTM based regulation as a means to increase the activity of the enolase enzyme. Our dataset also records only small upregulation for the pentose phosphate pathway enzymes phosphogluocono-lactonase (Tab. 1), this is in line with the small switch of carbon flows from glycolysis to the pentose phosphate pathway (PPP) [12]. The strongest impact of the mutation takes place in pyruvate metabolism as the pyruvate dehydrogenase subunit E1 is deleted in the *ΔaceE* strain. As a consequence of this pyruvate accumulation takes place and the carbon from glycolysis only directly enters the TCA through the pyruvate carboxylase reaction. Downregulation of enolase and phosphoglycerate dehydrogenase as well as deletion of the *aceE* gene impact the glycolytic pathway as more glucose is converted into pyruvate to feed the pyruvate carboxylase reaction as well as BCAA biosynthesis.

Our data provides an insight into fundamental changes of the carbon metabolism in *C. glutamicum* deficient of the pyruvate dehydrogenase function. To counter the lack of acetyl CoA resulting from the deletion of the PDHC E1 enzyme, BCAA production is coordinated with upregulation of the glyoxylate cycle and TCA cycle. The inability of the mutant to refill the TCA

cycle via pyruvate decarboxylation leads to the uptake of acetate via alternative pathways as SCOA. For provision of TCA cycle intermediates the glyoxylate cycle and pyruvate carboxylase pathway are activated. The accumulating pyruvate is converted to BCAA.

CONCLUSION

In this study, it was shown that the combination of FACS and proteomics is suitable for the selection and molecular characterization of microbial cells differing in the concentration of metabolites. In conclusion, we could demonstrate that small cell number proteomics is able to compare a BCAA producing strain and the WT after FACS sorting and exemplify the effect of deletion of a central step in carbon metabolism on the physiology of *C. glutamicum*. The used technology could enable proteomic characterization of biotechnologically significant emergence of a fast growing, non-productive subpopulation.

ACKNOWLEDGEMENTS

We are grateful to the Federal Ministry of Education and Research (BMBF) for generous financial support in the FlexFit initiative (0315589A as well as 0315589E). Furthermore we thank Julia Frunzke, Regina Mahr and Andrea Neumeyer from Research center Jülich for provision of samples and help with sample preparation. Also we thank Nils Bardeck for providing information on the protein content of single *C. glutamicum* cells.

Figures:

Fig. 1: Identified proteins relating to the applied cell number of *C. glutamicum* ATCC 13032 wild type. 100,000 cells and 1,000,000 cells were measured in two technical replicates, the means of both replicates being presented, while for 10,000 cells three technical replicates were measured. In three technical replicates an LC/MS method with an increased filling time and a higher number of fragmented peptides enabled identification of up to 800 proteins and a mean protein identification number of 650 proteins was achieved.

Fig. 2: a) Schematic view of experimental procedures for cell selection and sorting. *C. glutamicum ATCC13032* as well as a *C. glutamicum ΔaceE* with integrated LRP sensor were grown in CGXII medium containing 4% glucose and 1.5 % potassium acetate. Cells from both cultures were mixed together 1:1 after 12 hours growth time, then a FACS Aria II cell sorter was used to identify and sort cells based on the emergence of eYFP fluorescence in the *ΔaceE* cells (green). b) Sorting of cells presented by correlation of forward cell scatter and eYFP fluorescence for the WT and *ΔaceE* strain. c) Principal component analysis of the *C. glutamicum* ATCC 13032 and *C. glutamicum ΔaceE* proteomes. Principal component analysis was performed for z standardized proteome datasets for *C. glutamicum* ATCC 13032 cells and *C. glutamicum ΔaceE* cells acquired by FACS-sorting from a mixture and from each of the cultures before mixing. The red arrows indicate the directions of the proteome datasets in regards to the principal components

Fig. 3: a) Schematic presentation of enzymes (squares) involved in glycolysis and valine (BCAA) production**.** Arrows represent enzymes in the *C. glutamicum ΔaceE* and the *C. glutamicum ATCC 13032* strain. Enzyme names are given in squares. The regulation factor of up- or downregulation of enzymes in the *ΔaceE* mutant is represented by the color of the squares adjacent to the enzyme names as indicated in the color scale. Enzymes displayed in this figure are: HK = hexokinase, TPI = triose phosphate isomerase, GAP = glyceraldehyde-3-phosphate dehydrogenase, PHGDH = phosphoglycerate dehydrogenase, PGM = phosphoglycerate mutase, ENO = enolase, PYK = pyruvate kinase, ILVB = acetolactate synthase, DHAD = dihydroxyacid dehydratase, AceE = pyruvate:dehydrogenase complex. b) Schematic presentation of enzymes (squares) involved in Tricarboxylic acid cycle (TCA) and the glyoxylate cycle. Regulation factor of up- or downregulation of enzymes in the *ΔaceE* mutant is represented by the color of the squares adjacent to the enzyme names as indicated in the color scale.

Enzymes displayed in this figure are: MDH = malate dehydrogenase, CS = citrate synthase, ACO = aconitase, IDH = isocitrate dehydrogenase, IL = isocitrate lyase, MS = malate synthase, KGD = α-ketoglutarate-dehydrogenase, SCOA = succinyl acetate CoA transferase, SUC = succinyl CoA synthetase, SDH = succinate dehydrogenase, FUM = fumarase.

Supp. Fig. 1: Volcano Plots calculated for WT and *ΔaceE*. Log(2) logarithmized regulation factors were plotted against the –log10 P-values for every protein identified in WT and *ΔaceE.* Cutoff for significant regulation was set to 0.05.

Tables:

Table 1: Selection of physiologically important enzymes identified in the ΔaceE and WT *strains as showing significant regulation. Significant abundance changes of enzymes between strains are given as p-values obtained from ANOVA. The Regulation factor between the WT and ΔaceE (WT log2 area values subtracted from the ΔaceE log2 area values) was determined from the z-normalized area values for* WT *and ΔaceE samples. As threshold for significant regulation of proteins between strains a p-value below 0.05 was set. All significantly regulated proteins between WT and ΔaceE can be found in suppl. Table 2.*

Gene ID	Description	P-value between strains	RF (Δ aceE)
Energy metabolism			
Cg3048	PHOSPHATE ACETYLTRANSFERASE	3.05E-04	1.09
Cg3047	ACETATE KINASE	2.55E-03	0.87
Carbohydrate metabolism			
Cg0949	CITRATE SYNTHASE	4.12E-09	0.83
Cg0790	DIHYDROLIPOAMIDE DEHYDROGENASE	1.54E-02	0.59
Cg0791	PYRUVATE CARBOXYLASE	1.44E-05	0.64
Cg1737	ACONITASE	3.39E-03	0.33
Cg0766	ISOCITRATE DEHYDROGENASE	5.04E-05	0.40
Cg2421	DIHYDROLIPOAMIDE SUCCINYLTRANSFERASE	2.92E-02	0.25
Cg2840	SUCCINYL ACETATE COA-TRANSFERASE	2.06E-03	0.44
Cg0446	SUCCINATE DEHYDROGENASE A	4.47E-02	0.35
Cg1280	KETOGLUTARATE DEHYDROGENASE	2.70E-04	0.39
Cg1145	FUMARASE	8.32E-04	-0.39
Cg2613	MALATE DEHYDROGENASE	4.94E-04	-0.39
Cg1075	PHOSPHORIBOSYL PYROPHOSPHATE SYNTHASE	1.15E-02	0.36
Cg1780	PUTATIVE 6-PHOSPHOGLUCONOLACTONASE	5.45E-05	1.00
Cg2559	MALATE SYNTHASE	6.65E-04	0.53
Cg2192	MALATE:QUINONE OXIDOREDUCTASE	3.89E-02	0.24
Cg2521	LONG-CHAIN FATTY ACID COA LIGASE	4.74E-04	0.67
Cg0825	SHORT CHAIN DEHYDROGENASE; N-TERMINAL FRAGMENT	2.40E-04	1.01
Cg1373	GLYOXALASE	7.71E-04	-0.56
Cg0811	ACETYL/PROPIONYL COA CARBOXYLASE,	1.21E-04	0.35
Cg2560	ISOCITRATE LYASE	2.44E-07	1.13
Cg0802	BIOTIN CARBOXYLASE	3.02E-04	0.35
Cg1726	METHYLMALONYL-COA MUTASE	4.25E-02	0.33
Cg2091	POLYPHOSPHATE GLUCOKINASE	9.10E-03	0.63
Cg1268	GLYCOSYL TRANSFERASE	3.38E-02	0.34
Cg1381	1,4-ALPHA-GLUCAN BRANCHING ENZYME	1.63E-02	0.41
Cg2323	MALTOOLIGOSYL TREHALOSE SYNTHASE	2.50E-02	0.48
Cg1111	ENOLASE (2-PHOSPHOGLYCERATE DEHYDRATASE)	6.76E-04	-0.33
Cg1791	GLYCERALDEHYDE-3-PHOSPHATE DEHYDROGENASE	2.17E-02	-0.15
Nucleotide and amino acid metabolism			
Cg0703	PUTATIVE GMP SYNTHASE	3.26E-02	0.28
Cg0700	IMP DEHYDROGENASE / GMP REDUCTASE	2.36E-02	0.57
Cg2964	INOSITOL-MONOPHOSPHATE DEHYDROGENASE	6.12E-03	0.54
Cg2953	BENZALDEHYDE DEHYDROGENASE	8.00E-07	1.39
Cg1581	GLUTAMATE N-ACETYLTRANSFERASE	3.43E-04	0.63
Cg0490	PYRROLINE-5-CARBOXYLATE REDUCTASE	4.82E-03	0.37
Cg1451	PHOSPHOGLYCERATE DEHYDROGENASE	5.29E-05	-0.41
Cg2586	GAMMA-GLUTAMYL PHOSPHATE REDUCTASE	1.91E-07	0.90
Cg1453	3-ISOPROPYLMALATE DEHYDROGENASE	3.91E-02	0.38
Cg1488	3-ISOPROPYLMALATE DEHYDRATASE	4.64E-02	0.22
Cg0303	2-ISOPROPYLMALATE SYNTHASE	1.03E-03	1.11
Cg1432	DIHYDROXY-ACID DEHYDRATASE	5.09E-04	0.35
Cg1436	ACETOHYDROXYACID SYNTHASE SMALL SUBUNIT	1.18E-03	0.48
Cg1435	ACETOLACTATE SYNTHASE	1.03E-03	0.58
Cg1806	S-ADENOSYLMETHIONINE SYNTHETASE	3.40E-02	0.76
Cg0860	ADENOSYLHOMOCYSTEINASE	9.84E-03	0.77
Cg2833	O-ACETYLSERINE (THIOL)-LYASE	8.66E-05	0.26
Cg2437	THREONINE SYNTHASE	4.78E-03	0.40
Cg1338	HOMOSERINE KINASE	3.54E-03	0.57
Cg1337	HOMOSERINE DEHYDROGENASE	3.36E-04	0.60
Cg2779	PHOSPHOSERINE PHOSPHATASE	2.87E-02	0.34
Cg1713	DIHYDROOROTATE DEHYDROGENASE	1.53E-02	0.30
Cg2779	PHOSPHOSERINE PHOSPHATASE	2.87E-02	0.03
Cg1713	DIHYDROOROTATE DEHYDROGENASE	1.53E-02	0.06

Supplementary Table 1: Proteins identified as significantly regulated between mixed and separated samples of WT and ΔaceE strain cells. Significant regulation of a protein between mixed and separated cells is given in the p-value and the Benjamini&Hochberg corrected adjusted p-value. The Regulation factor (RF) of a protein for the mixed samples (values of the

separated values are subtracted from the values of the mixed samples) was determined from the z-normalized log2 area values of the separated and mixed samples from each strain. The threshold for significant regulation of proteins was set at a p-value of 0.05.

528

Gene names	Description	P-value mix	adj. P-value mix	RF mix/separated (WT)	RF mix/separated (Δ aceE)
Cg2994	PUTATIVE OR SECRETED MEMBRANE PROTEIN	1.79E-05	1.30E-02	NA	0.60
Cg3011	GROEL2 CHAPERONIN	1.07E-03	2.43E-01	-0.38	-0.21
Cg3306	50S RIBOSOMAL PROTEIN L9	1.47E-03	2.43E-01	-0.40	-0.21
Cg1560	EXCINUCLEASE ATPASE SUBUNIT	2.57E-03	2.43E-01	NA	0.51
Cg1841	PROBABLE ASPARTYL-TRNA SYNTHETASE	2.59E-03	2.43E-01	-0.87	-0.38
Cg3032	PUTATIVE SECRETED PROTEIN	2.89E-03	2.43E-01	-0.89	-0.31
Cg0414	CELL SURFACE POLYSACCHARIDE BIOSYNTHESIS	3.13E-03	2.43E-01	0.24	0.68
Cg0867	RIBOSOME-ASSOCIATED PROTEIN Y	3.14E-03	2.43E-01	0.24	0.68
Cg1476	THIAMINE BIOSYNTHESIS PROTEIN	3.16E-03	2.43E-01	0.77	0.18
Cg0842	PUTATIVE DNA HELICASE	3.86E-03	2.43E-01	0.52	0.55
Cg1206	PEP PHOSPHONOMUTASE	3.97E-03	2.43E-01	-0.41	-0.46
Cg0239	HYPOTHETICAL PROTEIN	4.29E-03	2.43E-01	NA	-0.73
Cg1853	GLYCEROL-3-PHOSPHATE DEHYDROGENASE	4.46E-03	2.43E-01	NA	0.80
Cg1362	ATP SYNTHASE F0 SUBUNIT 6	5.03E-03	2.43E-01	0.38	1.05
Cg2835	Predicted acetyltransferase	6.36E-03	2.43E-01	-0.47	-0.23
Cg2120	SUGAR SPECIFIC PTS SYSTEM	6.46E-03	2.43E-01	-0.68	-0.33
Cg2705	MALTOSE-BINDING PROTEIN PRECURSOR	6.82E-03	2.43E-01	0.17	0.65
Cg2647	TRIGGER FACTOR	7.09E-03	2.43E-01	-0.43	-0.20
Cg1437	KETOL-ACID REDUCTOISOMERASE ILVC	7.68E-03	2.43E-01	-0.34	-0.19
Cg2137	GLUTAMATE SECRETED BINDING PROTEIN	8.54E-03	2.43E-01	0.93	NA
Cg1780	PUTATIVE 6-PHOSPHOGLUCONOLACTONASE	8.56E-03	2.43E-01	-0.47	-0.43
Cg1763	UNCHARACTERIZED IRON-REGULATED ABC-TYPE TRANSPO	8.91E-03	2.43E-01	-0.63	-0.31
Cg0648	ADENYLATE KINASE	8.94E-03	2.43E-01	-0.28	-0.14
Cg2263	HYPOTHETICAL PROTEIN	9.00E-03	2.43E-01	NA	1.06
Cg1859	PUTATIVE SECRETED PROTEIN	9.93E-03	2.43E-01	-0.15	-0.44
Cg1333	ARGINYL-TRNA SYNTHETASE	1.05E-02	2.43E-01	-0.62	-0.22
Cg1538	DEPHOSPHO-COA KINASE	1.10E-02	2.43E-01	-0.59	-0.42
Cg2052	PUTATIVE SECRETED PROTEIN	1.13E-02	2.43E-01	-0.32	-0.94
Cg2026	HYPOTHETICAL PROTEIN	1.14E-02	2.43E-01	-1.09	-0.42
Cg2964	INOSITOL-MONOPHOSPHATE DEHYDROGENASE	1.17E-02	2.43E-01	-0.41	-0.39
Cg2911	ABC-TYPE MN/ZN TRANSPORT SYSTEM	1.19E-02	2.43E-01	0.19	1.67
Cg2873	PROLYL OLIGOPEPTIDASE	1.21E-02	2.43E-01	-0.97	-0.33
Cg0834	BACTERIAL EXTRACELLULAR SOLUTE-BINDING PROTEIN	1.23E-02	2.43E-01	0.27	0.49
Cg0007	DNA GYRASE SUBUNIT B	1.23E-02	2.43E-01	-0.49	-0.23
Cg0947	HYPOTHETICAL PROTEIN	1.25E-02	2.43E-01	-0.88	-0.38

Gene names	Description	P-value mix	adj. P-value mix	RF mix/separated (WT)	RF mix/separated (Δ aceE)
Cg3047	ACETATE KINASE	1.27E-02	2.43E-01	-0.62	-0.63
Cg1872	HYPOTHETICAL PROTEIN	1.27E-02	2.43E-01	-0.34	-0.08
Cg2521	LONG-CHAIN FATTY ACID COA LIGASE	1.27E-02	2.43E-01	0.1	0.36
Cg1588	ARGININOSUCCINATE LYASE	1.35E-02	2.48E-01	-0.56	-0.21
Cg0307	ASPARTATE-SEMIALDEHYDE DEHYDROGENASE	1.40E-02	2.48E-01	-0.48	-0.42
Cg2800	PHOSPHOGLUCOMUTASE	1.41E-02	2.48E-01	-0.39	-0.2
Cg1580	N-ACETYL-GAMMA-GLUTAMYL-PHOSPHATE REDUCTASE	1.45E-02	2.48E-01	-0.48	-0.56
Cg3132	PUTATIVE MEMBRANE PROTEIN	1.59E-02	2.48E-01	-0.34	-0.33
Cg1825	TRANSLATION ELONGATION FACTOR P	1.60E-02	2.48E-01	-0.28	-0.2
Cg2419	LEUCINE AMINOPEPTIDASE	1.63E-02	2.48E-01	-1.28	-0.33
Cg1586	ARGININOSUCCINATE SYNTHASE	1.63E-02	2.48E-01	-0.33	-0.47
Cg0691	60 KDA CHAPERONIN	1.64E-02	2.48E-01	-0.2	-0.23
Cg1487	3-ISOPROPYLMALATE DEHYDRATASE LARGE SUBUNIT	1.67E-02	2.48E-01	-0.57	-0.53
Cg2310	GLYCOGEN DEBRANCHING ENZYME	1.68E-02	2.48E-01	NA	-0.77
Cg0576	DNA-DIRECTED RNA POLYMERASE BETA CHAIN	1.84E-02	2.66E-01	-0.32	-0.1
Cg1463	PUTATIVE GLUTAMYL-TRNA SYNTHETASE	1.94E-02	2.72E-01	-0.7	-0.23
Cg2863	PHOSPHORIBOSYLFORMYL GLYCINAMIDINE SYNTHASE	1.98E-02	2.72E-01	-0.51	-0.4
Cg2102	RNA POLYMERASE SIGMA FACTOR	1.99E-02	2.72E-01	NA	-0.35
Cg1764	UNCHARACTERIZED IRON-REGULATED ABC-TYPE TRANSPORTER	2.15E-02	2.87E-01	-0.64	-0.31
Cg1404	PROBABLE GLU-TRNA AMIDOTRANSFERASE	2.18E-02	2.87E-01	-0.42	-0.24
Cg1531	Zn-DEPENDENT HYDROLASE	2.39E-02	3.03E-01	-0.27	-0.13
Cg2611	MOLECULAR CHAPERONE, HSP 70 FAMILY	2.39E-02	3.03E-01	NA	0.85
Cg1270	PROBABLE O-METHYLTRANSFERASE	2.50E-02	3.04E-01	NA	-0.35
Cg2954	CARBONIC ANHYDRASE	2.52E-02	3.04E-01	0.22	0.29
Cg2499	GLYCYL-TRNA SYNTHETASE	2.61E-02	3.04E-01	-0.43	-0.16
Cg2833	O-ACETYLSERINE THIOL LYASE	2.64E-02	3.04E-01	-0.13	-0.14
Cg1867	PREPROTEIN TRANSLOCASE SUBUNIT SECD	2.65E-02	3.04E-01	NA	0.52
Cg2661	PUTATIVE DITHIOL-DISULFIDE ISOMERASE	2.73E-02	3.04E-01	0.21	0.22
Cg3169	PROBABLE PHOSPHOENOLPYRUVATE CARBOXYKINASE PROTEIN	2.73E-02	3.04E-01	-0.31	-0.17
Cg2456	ZN-RIBBON PROTEIN	2.76E-02	3.04E-01	-0.22	-0.35
Cg0825	SHORT CHAIN DEHYDROGENASE	2.77E-02	3.04E-01	-1.14	-0.09

Gene names	Description	P-value mix	adj. P-value mix	RF mix/separated (WT)	RF mix/separated (Δ aceE)
Cg0790	DIHYDROLIPOAMIDE DEHYDROGENASE	2.88E-02	3.04E-01	-0.50	-0.34
Cg3182	TREHALOSE CORYNOMYCOLYL TRANSFERASE	2.89E-02	3.04E-01	0.10	0.76
Cg2217	RIBOSOME RECYCLING FACTOR	2.93E-02	3.04E-01	-0.28	-0.08
Cg2117	PHOSPHOENOLPYRUVATE PHOSPHOTRANSFERASE SYSTEM	2.98E-02	3.04E-01	-0.33	-0.19
Cg2953	BENZALDEHYDE DEHYDROGENASE	2.98E-02	3.04E-01	-0.67	-0.12
Cg0387	PUTATIVE ZINC-TYPE ALCOHOL DEHYDROGENASE	3.03E-02	3.04E-01	-0.39	-0.23
Cg3050	ACYLTRANSFERASE	3.16E-02	3.09E-01	-0.48	-0.45
Cg0424	PUTATIVE GLYCOSYLTRANSFERASE	3.17E-02	3.09E-01	NA	0.53
Cg1574	PHENYLALANYL-TRNA SYNTHETASE ALPHA CHAIN	3.21E-02	3.09E-01	-0.94	-0.11
Cg2366	CELL DIVISION GTPASE	3.29E-02	3.13E-01	-0.27	-0.31
Cg0625	SECRETED PROTEIN	3.32E-02	3.13E-01	-0.44	-0.20
Cg2273	RIBONUCLEASE III	3.54E-02	3.15E-01	NA	-0.34
Cg2359	ISOLEUCINE-TRNA LIGASE-LIKE PROTEIN	3.62E-02	3.15E-01	-0.90	-0.16
Cg2963	PROBABLE ATP-DEPENDENT PROTEASE	3.64E-02	3.15E-01	-0.33	-0.10
Cg1880	THREONYL-TRNA SYNTHETASE	3.64E-02	3.15E-01	-0.34	-0.25
Cg2141	DNA RECOMBINATION/REPAIR	3.64E-02	3.15E-01	-0.49	-0.16
Cg1075	PHOSPHORIBOSYL PYROPHOSPHATE SYNTHASE ISOZYME	3.69E-02	3.15E-01	-0.31	-0.21
Cg2437	THREONINE SYNTHASE	3.70E-02	3.15E-01	-0.39	-0.11
Cg0438	PUTATIVE GLYCOSYLTRANSFERASE	3.70E-02	3.15E-01	0.19	0.71
Cg2363	HYPOTHETICAL PROTEIN	3.79E-02	3.19E-01	-0.94	-0.29
Cg2221	TRANSLATION ELONGATION FACTOR TS	3.89E-02	3.24E-01	-0.24	-0.31
Cg0193	ENDOPEPTIDASE O	3.97E-02	3.24E-01	-0.50	-0.41
Cg0766	ISOCITRATE DEHYDROGENASE	3.98E-02	3.24E-01	-0.14	-0.17
Cg0594	50S RIBOSOMAL PROTEIN L3	4.15E-02	3.32E-01	-0.38	-0.19
Cg1236	THIOL PEROXIDASE	4.17E-02	3.32E-01	-0.57	-0.10
Cg0807	HYPOTHETICAL PROTEIN	4.33E-02	3.41E-01	-1.00	-0.28
Cg3178	POLYKETIDE SYNTHASE	4.61E-02	3.57E-01	-0.75	-0.02
Cg3049	PUTATIVE FERREDOXIN/FERREDOXIN-NADP REDUCTASE	4.64E-02	3.57E-01	-0.76	-0.43
Cg0791	PYRUVATE CARBOXYLASE	4.75E-02	3.60E-01	-0.22	-0.20
Cg1365	H+-ATPASE DELTA SUBUNIT	4.81E-02	3.60E-01	0.35	0.23
Cg1228	ABC-type cobalt transport system, ATPase component	4.99E-02	3.60E-01	-0.72	-0.03

Supplementary Table 2: Proteins identified as significantly regulated between mixed and separated samples of WT and ΔaceE strain cells. Significant regulation of a protein between WT and ΔaceE strains cells is given in the p-value and the Benjamini&Hochberg corrected adjusted p-value. The Regulation factor (RF) of a protein (z-normalized log2 WT values are subtracted from the z-normalized log2 ΔaceE values) was determined from the area values of each strain combining the separated and mixed samples. For each strain also the combined number of unique peptides from mixed and separated samples is given. The threshold for significant regulation of proteins was set at a p-value of 0.05.

References

[1] Franz AK, Danielewicz MA, Wong DM, Anderson LA, Boothe JR. Phenotypic screening with oleaginous microalgae reveals modulators of lipid productivity. ACS Chem Biol 2013;8(5):1053–62.

[2] Mustafi N, Grünberger A, Kohlheyer D, Bott M, Frunzke J. The development and application of a single-cell biosensor for the detection of l-methionine and branched-chain amino acids. Metab. Eng. 2012;14(4):449–57.

[3] Fritzsch FSO, Dusny C, Frick O, Schmid A. Single-cell analysis in biotechnology, systems biology, and biocatalysis. Annu Rev Chem Biomol Eng 2012;3:129–55.

[4] Valet G. Cytomics: An entry to biomedical cell systems biology. Cytometry 2005;63A(2):67–8.

[5] Wiacek C, Müller S, Benndorf D. A cytomic approach reveals population heterogeneity of *Cupriavidus necator* in response to harmful phenol concentrations. Proteomics 2006;6(22):5983–94.

[6] Jehmlich N, Hübschmann T, Gesell Salazar M, Völker U, Benndorf D, Müller S et al. Advanced tool for characterization of microbial cultures by combining cytomics and proteomics. Applied Microbiology and Biotechnology 2010;88(2):575–84.

[7] Eggeling L, Bott M. Handbook of *Corynebacterium Glutamicum*. Boca Raton: Taylor & Francis; 2005.

[8] Becker J, Wittmann C. Bio-based production of chemicals, materials and fuels - *Corynebacterium glutamicum* as versatile cell factory. Curr. Opin. Biotechnol. 2012;23(4):631–40.

[9] Kennerknecht N, Sahm H, Yen, Patek M, Saier MH, Eggeling L. Export of L-isoleucine from *Corynebacterium glutamicum*: a Two-Gene-Encoded Member of a New Translocator Family. Journal of Bacteriology 2002;184(14):3947–56.

[10] Blombach B, Schreiner ME, Holátko J, Bartek T, Oldiges M, Eikmanns BJ. L-valine production with pyruvate dehydrogenase complex-deficient *Corynebacterium glutamicum*. Applied and Environmental Microbiology 2007;73(7):2079–84.

[11] Bartek T, Rudolf C, Kerssen U, Klein B, Blombach B, Lang S et al. Studies on substrate utilisation in L-valine-producing *Corynebacterium glutamicum* strains deficient in pyruvate dehydrogenase complex. Bioprocess Biosyst Eng 2010;33(7):873–83.

[12] Bartek T, Blombach B, Lang S, Eikmanns BJ, Wiechert W, Oldiges M et al. Comparative ^{13}C metabolic flux analysis of pyruvate dehydrogenase complex-deficient, L-valine-

producing *Corynebacterium glutamicum*. Appl. Environ. Microbiol. 2011;77(18):6644–52.
[13] Kalinowski J, Bathe B, Bartels D, Bischoff N, Bott M, Burkovski A et al. The complete *Corynebacterium glutamicum* ATCC 13032 genome sequence and its impact on the production of l-aspartate-derived amino acids and vitamins. Journal of Biotechnology 2003;104(1-3):5–25.
[14] Blombach B, Schreiner ME, Bartek T, Oldiges M, Eikmanns BJ. *Corynebacterium glutamicum* tailored for high-yield L-valine production. Applied Microbiology and Biotechnology 2008;79(3):471–9.
[15] Keilhauer C, Eggeling L, Sahm H. Isoleucine Synthesis in *Corynebacterium glutamicum*: Molecular Analysis of the ilvB-ilvN-ilvC Operon. Journal of Bacteriology 1993;175(17):5595–603.
[16] Liu H, Sadygov RG, Yates JR. A model for random sampling and estimation of relative protein abundance in shotgun proteomics. Anal. Chem. 2004;76(14):4193–201.
[17] Silva J, Gorenstein M, Li G-Z, Vissers J, Geromanos S. Absolute Quantification of Proteins by LCMS. Mol. Cell Proteomics 2006;2006(5):144–56.
[18] Carranza P, Grunau A, Schneider T, Hartmann I, Lehner A, Stephan R et al. A gel-free quantitative proteomics approach to investigate temperature adaptation of the food-borne pathogen *Cronobacter turicensis* 3032. Proteomics 2010;10(18):3248–61.
[19] Team TRC. R: A Language and Environment for Statistical Computing;2016.
[20] Cayley S, Lewis BA, Guttman HJ, Record M. Characterization of the cytoplasm of *Escherichia coli* K-12 as a function of external osmolarity. Journal of Molecular Biology 1991;222(2):281–300.
[21] Jahn M, Seifert J, Hübschmann T, Bergen M, Harms H, Müller S. Comparison of preservation methods for bacterial cells in cytomics and proteomics. JIOMICS 2013;3(1).
[22] Wendisch VF, Graaf AA, Sahm H, Eikmanns BJ. Quantitative Determination of Metabolic Fluxes during Coutilization of Two Carbon Sources: Comparative Analyses with *Corynebacterium glutamicum* during Growth on Acetate and/or Glucose. Journal of Bacteriology 2000;182(11):3088–96.
[23] Hayashi M, Mizoguchi H, SHIRAISHI N, OBAYASHI M, NAKAGAWA S, IMAI J-i et al. Transcriptome Analysis of Acetate Metabolism in *Corynebacterium glutamicum* Using a Newly Developed Metabolic Array: Bioscience, Biotechnology, and Biochemistry. Bioscience, Biotechnology and Biochemistry 2002;66(6):1337–44.
[24] Gerstmeir R, Wendisch VF, Schnicke S, Ruan H, Farwick M, Reinscheid D et al. Acetate metabolism and its regulation in *Corynebacterium glutamicum*. Journal of Biotechnology 2003;104(1-3):99–122.
[25] Gerstmeir R, Cramer A, Dangel P, Schaffer S, Eikmanns BJ. RamB, a Novel Transcriptional Regulator of Genes Involved in Acetate Metabolism of *Corynebacterium glutamicum*. Journal of Bacteriology 2004;186(9):2798–809.
[26] Veit A, Rittmann D, Georgi T, Youn J-W, Eikmanns BJ, Wendisch VF. Pathway identification combining metabolic flux and functional genomics analyses: acetate and propionate activation by *Corynebacterium glutamicum*. Journal of Biotechnology 2009;140(1-2):75–83.
[27] Voges R, Noack S. Quantification of proteome dynamics in *Corynebacterium glutamicum* by (15)N-labeling and selected reaction monitoring. J Proteomics 2012;75(9):2660–9.
[28] Leyval D, Uy D, Delaunay S, Goergen JL, Engasser JM. Characterisation of the enzyme activities involved in the valine biosynthetic pathway in a valine-producing strain of *Corynebacterium glutamicum*. Journal of Biotechnology 2003;104(1-3):241–52.

625

Table

Click here to download Table: Table1.xlsx

Gene ID	Description
Energy metabolism	
Cg3048	PHOSPHATE ACETYLTRANSFERASE
Cg3047	ACETATE KINASE
Carbohydrate metabolism	
Cg0949	CITRATE SYNTHASE
Cg0790	DIHYDROLIPOAMIDE DEHYDROGENASE
Cg0791	PYRUVATE CARBOXYLASE
Cg1737	ACONITASE
Cg0766	ISOCITRATE DEHYDROGENASE
Cg2421	DIHYDROLIPOAMIDE SUCCINYLTRANSFERASE
Cg2840	SUCCINYL ACETATE COA-TRANSFERASE
Cg0446	SUCCINATE DEHYDROGENASE A
Cg1280	KETOGLUTARATE DEHYDROGENASE
Cg1145	FUMARATE HYDRATASE
Cg2613	MALATE DEHYDROGENASE
Cg1075	PHOSPHORIBOSYL PYROPHOSPHATE SYNTHASE
Cg1780	PUTATIVE 6-PHOSPHOGLUCONOLACTONASE
Cg2559	MALATE SYNTHASE
Cg2192	MALATE:QUINONE OXIDOREDUCTASE
Cg2521	LONG-CHAIN FATTY ACID COA LIGASE
Cg0825	SHORT CHAIN DEHYDROGENASE; N-TERMINAL FRAGMENT
Cg1373	GLYOXALASE
Cg0811	ACETYL/PROPIONYL COA CARBOXYLASE,
Cg2560	ISOCITRATE LYASE
Cg0802	BIOTIN CARBOXYLASE
Cg1726	METHYLMALONYL-COA MUTASE
Cg2091	POLYPHOSPHATE GLUCOKINASE
Cg1268	GLYCOSYL TRANSFERASE
Cg1381	1,4-ALPHA-GLUCAN BRANCHING ENZYME
Cg2323	MALTOOLIGOSYL TREHALOSE SYNTHASE
Cg1111	ENOLASE (2-PHOSPHOGLYCERATE DEHYDRATASE)
Cg1069	GLYCERALDEHYDE-3-PHOSPHATE DEHYDROGENASE
Nucleotide and amino acid metabolism	
Cg0703	PUTATIVE GMP SYNTHASE
Cg0700	IMP DEHYDROGENASE / GMP REDUCTASE
Cg2964	INOSITOL-MONOPHOSPHATE DEHYDROGENASE
Cg2953	BENZALDEHYDE DEHYDROGENASE
Cg1581	GLUTAMATE N-ACETYLTRANSFERASE
Cg0490	PYRROLINE-5-CARBOXYLATE REDUCTASE
Cg1451	PHOSPHOGLYCERATE DEHYDROGENASE
Cg2586	GAMMA-GLUTAMYL PHOSPHATE REDUCTASE
Cg1453	3-ISOPROPYLMALATE DEHYDROGENASE
Cg1488	3-ISOPROPYLMALATE DEHYDRATASE
Cg0303	2-ISOPROPYLMALATE SYNTHASE
Cg1432	DIHYDROXY-ACID DEHYDRATASE
Cg1436	ACETOHYDROXYACID SYNTHASE SMALL SUBUNIT
Cg1435	ACETOHYDROXYACID SYNTHASE
Cg1806	S-ADENOSYLMETHIONINE SYNTHETASE

Figure
Click here to download Figure: Figure 1.eps

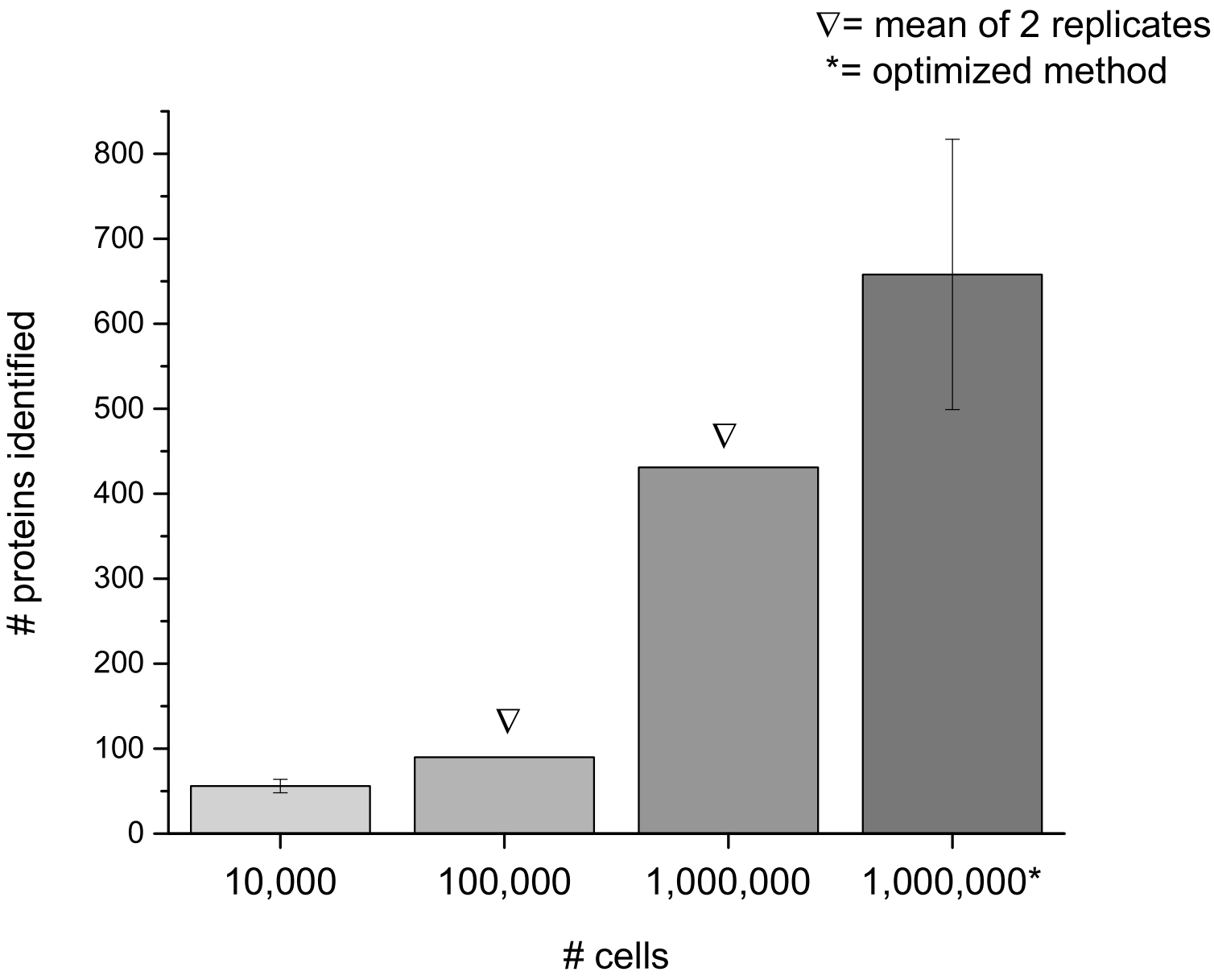

Figure

Click here to download high resolution image

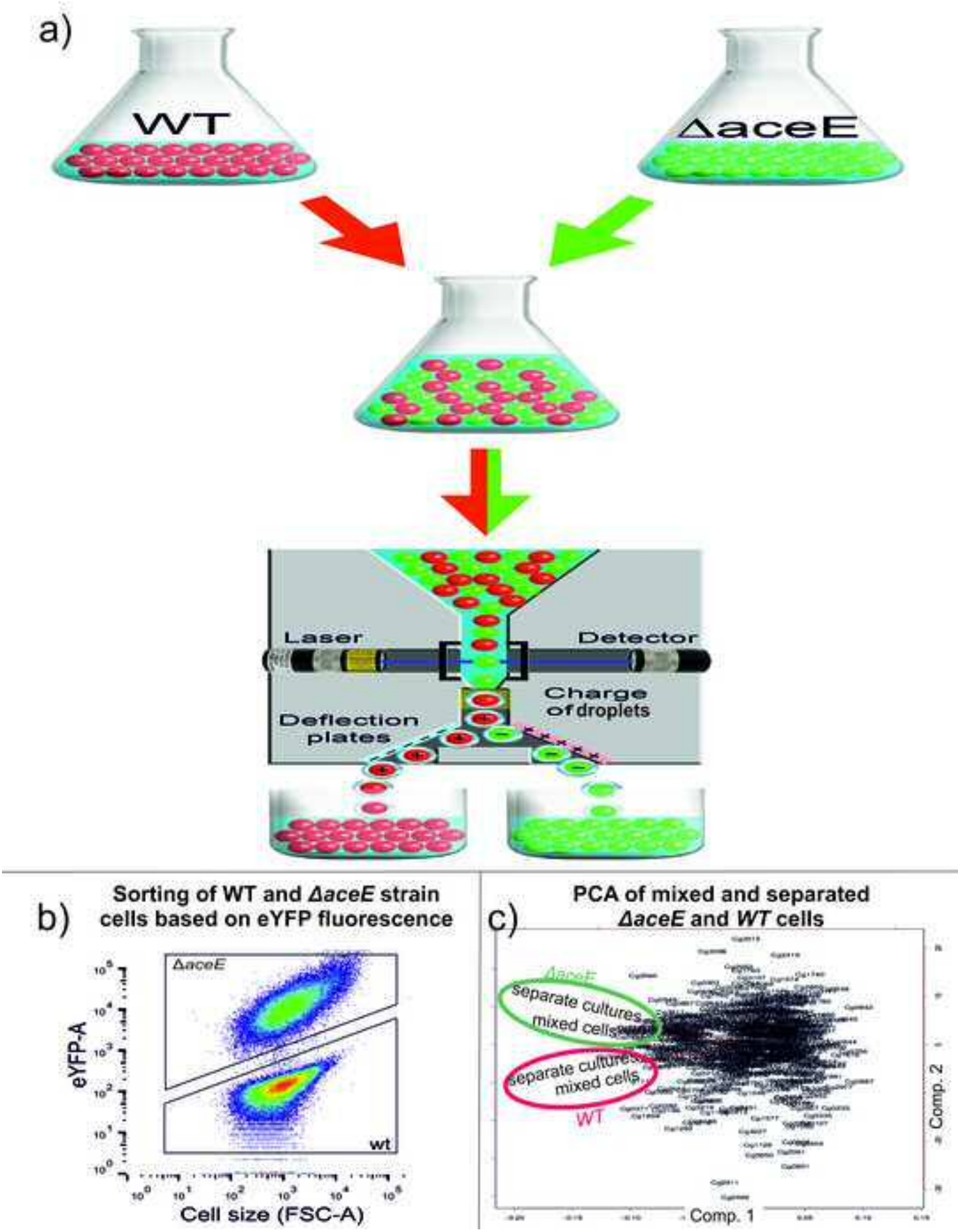

Figure
Click here to download Figure: Figure3.pptx